

Measurement of the Λ_b^0 Lifetime in $\Lambda_b^0 \rightarrow \Lambda_c^+ \pi^-$ Decays in $p\bar{p}$ Collisions at $\sqrt{s} = 1.96$ TeV

T. Aaltonen,²⁴ J. Adelman,¹⁴ B. Álvarez González^{v,12} S. Amerio^{dd,44} D. Amidei,³⁵ A. Anastassov,³⁹ A. Annovi,²⁰ J. Antos,¹⁵ G. Apollinari,¹⁸ A. Apresyan,⁴⁹ T. Arisawa,⁵⁸ A. Artikov,¹⁶ J. Asaadi,⁵⁴ W. Ashmanskas,¹⁸ A. Attal,⁴ A. Aurisano,⁵⁴ F. Azfar,⁴³ W. Badgett,¹⁸ A. Barbaro-Galtieri,²⁹ V.E. Barnes,⁴⁹ B.A. Barnett,²⁶ P. Barria^{ff,47} P. Bartos,¹⁵ G. Bauer,³³ P.-H. Beauchemin,³⁴ F. Bedeschi,⁴⁷ D. Beecher,³¹ S. Behari,²⁶ G. Bellettini^{ee,47} J. Bellinger,⁶⁰ D. Benjamin,¹⁷ A. Beretvas,¹⁸ A. Bhatti,⁵¹ M. Binkley,¹⁸ D. Bisello^{dd,44} I. Bizjak^{jj,31} R.E. Blair,² C. Blocker,⁷ B. Blumenfeld,²⁶ A. Bocci,¹⁷ A. Bodek,⁵⁰ V. Boisvert,⁵⁰ D. Bortoletto,⁴⁹ J. Boudreau,⁴⁸ A. Boveia,¹¹ B. Brau^{a,11} A. Bridgeman,²⁵ L. Brigliadori^{cc,6} C. Bromberg,³⁶ E. Brubaker,¹⁴ J. Budagov,¹⁶ H.S. Budd,⁵⁰ S. Budd,²⁵ K. Burkett,¹⁸ G. Busetto^{dd,44} P. Bussey,²² A. Buzatu,³⁴ K. L. Byrum,² S. Cabrera^{x,17} C. Calancha,³² S. Camarda,⁴ M. Campanelli,³¹ M. Campbell,³⁵ F. Canelli^{14,18} A. Canepa,⁴⁶ B. Carls,²⁵ D. Carlsmith,⁶⁰ R. Carosi,⁴⁷ S. Carrillo^{n,19} S. Carron,¹⁸ B. Casal,¹² M. Casarsa,¹⁸ A. Castro^{cc,6} P. Catastini^{ff,47} D. Cauz,⁵⁵ V. Cavaliere^{ff,47} M. Cavalli-Sforza,⁴ A. Cerri,²⁹ L. Cerrito^{q,31} S.H. Chang,²⁸ Y.C. Chen,¹ M. Chertok,⁸ G. Chiarelli,⁴⁷ G. Chlachidze,¹⁸ F. Chlebana,¹⁸ K. Cho,²⁸ D. Chokheli,¹⁶ J.P. Chou,²³ K. Chung^{o,18} W.H. Chung,⁶⁰ Y.S. Chung,⁵⁰ T. Chwalek,²⁷ C.I. Ciobanu,⁴⁵ M.A. Ciocci^{ff,47} A. Clark,²¹ D. Clark,⁷ G. Compostella,⁴⁴ M.E. Convery,¹⁸ J. Conway,⁸ M. Corbo,⁴⁵ M. Cordelli,²⁰ C.A. Cox,⁸ D.J. Cox,⁸ F. Crescioli^{ee,47} C. Cuenca Almenar,⁶¹ J. Cuevas^{v,12} R. Culbertson,¹⁸ J.C. Cully,³⁵ D. Dagenhart,¹⁸ M. Datta,¹⁸ T. Davies,²² P. de Barbaro,⁵⁰ S. De Cecco,⁵² A. Deisher,²⁹ G. De Lorenzo,⁴ M. Dell'Orso^{ee,47} C. Deluca,⁴ L. Demortier,⁵¹ J. Deng^{f,17} M. Deninno,⁶ M. d'Errico^{dd,44} A. Di Canto^{ee,47} G.P. di Giovanni,⁴⁵ B. Di Ruzza,⁴⁷ J.R. Dittmann,⁵ M. D'Onofrio,⁴ S. Donati^{ee,47} P. Dong,¹⁸ T. Dorigo,⁴⁴ S. Dube,⁵³ K. Ebina,⁵⁸ A. Elagin,⁵⁴ R. Erbacher,⁸ D. Errede,²⁵ S. Errede,²⁵ N. Ershaidat^{bb,45} R. Eusebi,⁵⁴ H.C. Fang,²⁹ S. Farrington,⁴³ W.T. Fedorko,¹⁴ R.G. Feild,⁶¹ M. Feindt,²⁷ J.P. Fernandez,³² C. Ferrazza^{gg,47} R. Field,¹⁹ G. Flanagan^{s,49} R. Forrest,⁸ M.J. Frank,⁵ M. Franklin,²³ J.C. Freeman,¹⁸ I. Furic,¹⁹ M. Gallinaro,⁵¹ J. Galyardt,¹³ F. Garbersen,¹¹ J.E. Garcia,²¹ A.F. Garfinkel,⁴⁹ P. Garosi^{ff,47} H. Gerberich,²⁵ D. Gerdes,³⁵ A. Gessler,²⁷ S. Giagu^{hh,52} V. Giakoumopoulou,³ P. Giannetti,⁴⁷ K. Gibson,⁴⁸ J.L. Gimmell,⁵⁰ C.M. Ginsburg,¹⁸ N. Giokaris,³ M. Giordani^{ii,55} P. Giromini,²⁰ M. Giunta,⁴⁷ G. Giurgiu,²⁶ V. Glagolev,¹⁶ D. Glenzinski,¹⁸ M. Gold,³⁸ N. Goldschmidt,¹⁹ A. Golossanov,¹⁸ G. Gomez,¹² G. Gomez-Ceballos,³³ M. Goncharov,³³ O. González,³² I. Gorelov,³⁸ A.T. Goshaw,¹⁷ K. Goulianos,⁵¹ A. Gresele^{dd,44} S. Grinstein,⁴ C. Grosso-Pilcher,¹⁴ R.C. Group,¹⁸ U. Grundler,²⁵ J. Guimaraes da Costa,²³ Z. Gunay-Unalan,³⁶ C. Haber,²⁹ S.R. Hahn,¹⁸ E. Halkiadakis,⁵³ B.-Y. Han,⁵⁰ J.Y. Han,⁵⁰ F. Happacher,²⁰ K. Hara,⁵⁶ D. Hare,⁵³ M. Hare,⁵⁷ R.F. Harr,⁵⁹ M. Hartz,⁴⁸ K. Hatakeyama,⁵ C. Hays,⁴³ M. Heck,²⁷ J. Heinrich,⁴⁶ M. Herndon,⁶⁰ J. Heuser,²⁷ S. Hewamanage,⁵ D. Hidas,⁵³ C.S. Hill^{c,11} D. Hirschbuehl,²⁷ A. Hocker,¹⁸ S. Hou,¹ M. Houlden,³⁰ S.-C. Hsu,²⁹ R.E. Hughes,⁴⁰ M. Hurwitz,¹⁴ U. Husemann,⁶¹ M. Hussein,³⁶ J. Huston,³⁶ J. Incandela,¹¹ G. Introzzi,⁴⁷ M. Iori^{hh,52} A. Ivanov^{p,8} E. James,¹⁸ D. Jang,¹³ B. Jayatilaka,¹⁷ E.J. Jeon,²⁸ M.K. Jha,⁶ S. Jindariani,¹⁸ W. Johnson,⁸ M. Jones,⁴⁹ K.K. Joo,²⁸ S.Y. Jun,¹³ J.E. Jung,²⁸ T.R. Junk,¹⁸ T. Kamon,⁵⁴ D. Kar,¹⁹ P.E. Karchin,⁵⁹ Y. Kato^{m,42} R. Kephart,¹⁸ W. Ketchum,¹⁴ J. Keung,⁴⁶ V. Khotilovich,⁵⁴ B. Kilminster,¹⁸ D.H. Kim,²⁸ H.S. Kim,²⁸ H.W. Kim,²⁸ J.E. Kim,²⁸ M.J. Kim,²⁰ S.B. Kim,²⁸ S.H. Kim,⁵⁶ Y.K. Kim,¹⁴ N. Kimura,⁵⁸ L. Kirsch,⁷ S. Klimentenko,¹⁹ K. Kondo,⁵⁸ D.J. Kong,²⁸ J. Konigsberg,¹⁹ A. Korytov,¹⁹ A.V. Kotwal,¹⁷ M. Kreps,²⁷ J. Kroll,⁴⁶ D. Krop,¹⁴ N. Krumnack,⁵ M. Kruse,¹⁷ V. Krutelyov,¹¹ T. Kuhr,²⁷ N.P. Kulkarni,⁵⁹ M. Kurata,⁵⁶ S. Kwang,¹⁴ A.T. Laasanen,⁴⁹ S. Lami,⁴⁷ S. Lammel,¹⁸ M. Lancaster,³¹ R.L. Lander,⁸ K. Lannon^{u,40} A. Lath,⁵³ G. Latino^{ff,47} I. Lazzizzera^{dd,44} T. LeCompte,² E. Lee,⁵⁴ H.S. Lee,¹⁴ J.S. Lee,²⁸ S.W. Lee^{w,54} S. Leone,⁴⁷ J.D. Lewis,¹⁸ C.-J. Lin,²⁹ J. Linacre,⁴³ M. Lindgren,¹⁸ E. Lipeles,⁴⁶ A. Lister,²¹ D.O. Litvintsev,¹⁸ C. Liu,⁴⁸ T. Liu,¹⁸ N.S. Lockyer,⁴⁶ A. Loginov,⁶¹ L. Lovas,¹⁵ D. Lucchesi^{dd,44} J. Lueck,²⁷ P. Lujan,²⁹ P. Lukens,¹⁸ G. Lungu,⁵¹ J. Lys,²⁹ R. Lysak,¹⁵ D. MacQueen,³⁴ R. Madrak,¹⁸ K. Maeshima,¹⁸ K. Makhoul,³³ P. Maksimovic,²⁶ S. Malde,⁴³ S. Malik,³¹ G. Manca^{e,30} A. Manousakis-Katsikakis,³ F. Margaroli,⁴⁹ C. Marino,²⁷ C.P. Marino,²⁵ A. Martin,⁶¹ M.S. Martin,²⁶ V. Martin^{k,22} M. Martínez,⁴ R. Martínez-Ballarín,³² P. Mastrandrea,⁵² M. Mathis,²⁶ M.E. Mattson,⁵⁹ P. Mazzanti,⁶ K.S. McFarland,⁵⁰ P. McIntyre,⁵⁴ R. McNulty^{j,30} A. Mehta,³⁰ P. Mehtala,²⁴ A. Menzione,⁴⁷ C. Mesropian,⁵¹ T. Miao,¹⁸ D. Mietlicki,³⁵ N. Miladinovic,⁷ R. Miller,³⁶ C. Mills,²³ M. Milnik,²⁷ A. Mitra,¹ G. Mitselmakher,¹⁹ H. Miyake,⁵⁶ S. Moed,²³ N. Moggi,⁶ M.N. Mondragon^{n,18} C.S. Moon,²⁸ R. Moore,¹⁸ M.J. Morello,⁴⁷ J. Morlock,²⁷ P. Movilla Fernandez,¹⁸ J. Müllenstädt,²⁹ A. Mukherjee,¹⁸ Th. Müller,²⁷ R. Mumford,²⁶ P. Murat,¹⁸ M. Mussini^{cc,6} J. Nachtman^{o,18} Y. Nagai,⁵⁶ J. Naganoma,⁵⁶ K. Nakamura,⁵⁶ I. Nakano,⁴¹ A. Napier,⁵⁷ J. Nett,⁶⁰ C. Neu^{z,46} M.S. Neubauer,²⁵ S. Neubauer,²⁷ J. Nielsen^{g,29} L. Nodulman,² M. Norman,¹⁰ O. Norniella,²⁵ E. Nurse,³¹ L. Oakes,⁴³ S.H. Oh,¹⁷ Y.D. Oh,²⁸ I. Oksuzian,¹⁹ T. Okusawa,⁴²

R. Orava,²⁴ K. Osterberg,²⁴ S. Pagan Griso^{dd,44} C. Pagliarone,⁵⁵ E. Palencia,¹⁸ V. Papadimitriou,¹⁸ A. Papaikononou,²⁷ A.A. Paramanov,² B. Parks,⁴⁰ S. Pashapour,³⁴ J. Patrick,¹⁸ G. Pauletta^{ii,55} M. Paulini,¹³ C. Paus,³³ T. Peiffer,²⁷ D.E. Pellett,⁸ A. Penzo,⁵⁵ T.J. Phillips,¹⁷ G. Piacentino,⁴⁷ E. Pianori,⁴⁶ L. Pinera,¹⁹ K. Pitts,²⁵ C. Plager,⁹ L. Pondrom,⁶⁰ K. Potamianos,⁴⁹ O. Poukhov*,¹⁶ F. Prokoshin^{y,16} A. Pronko,¹⁸ F. Ptohos^{i,18} E. Pueschel,¹³ G. Punzi^{ee,47} J. Pursley,⁶⁰ J. Rademacker^{c,43} A. Rahaman,⁴⁸ V. Ramakrishnan,⁶⁰ N. Ranjan,⁴⁹ I. Redondo,³² P. Renton,⁴³ M. Renz,²⁷ M. Rescigno,⁵² S. Richter,²⁷ F. Rimondi^{cc,6} L. Ristori,⁴⁷ A. Robson,²² T. Rodrigo,¹² T. Rodriguez,⁴⁶ E. Rogers,²⁵ S. Rolli,⁵⁷ R. Roser,¹⁸ M. Rossi,⁵⁵ R. Rossin,¹¹ P. Roy,³⁴ A. Ruiz,¹² J. Russ,¹³ V. Rusu,¹⁸ B. Rutherford,¹⁸ H. Saarikko,²⁴ A. Safonov,⁵⁴ W.K. Sakumoto,⁵⁰ L. Santi^{ii,55} L. Sartori,⁴⁷ K. Sato,⁵⁶ A. Savoy-Navarro,⁴⁵ P. Schlabach,¹⁸ A. Schmidt,²⁷ E.E. Schmidt,¹⁸ M.A. Schmidt,¹⁴ M.P. Schmidt*,⁶¹ M. Schmitt,³⁹ T. Schwarz,⁸ L. Scodellaro,¹² A. Scribano^{ff,47} F. Scuri,⁴⁷ A. Sedov,⁴⁹ S. Seidel,³⁸ Y. Seiya,⁴² A. Semenov,¹⁶ L. Sexton-Kennedy,¹⁸ F. Sforza^{ee,47} A. Sfyrla,²⁵ S.Z. Shalhout,⁵⁹ T. Shears,³⁰ P.F. Shepard,⁴⁸ M. Shimojima^{t,56} S. Shiraishi,¹⁴ M. Shochet,¹⁴ Y. Shon,⁶⁰ I. Shreyber,³⁷ A. Simonenko,¹⁶ P. Sinervo,³⁴ A. Sisakyan,¹⁶ A.J. Slaughter,¹⁸ J. Slaunwhite,⁴⁰ K. Sliwa,⁵⁷ J.R. Smith,⁸ F.D. Snider,¹⁸ R. Snihur,³⁴ A. Soha,¹⁸ S. Somalwar,⁵³ V. Sorin,⁴ P. Squillacioti^{ff,47} M. Stanitzki,⁶¹ R. St. Denis,²² B. Stelzer,³⁴ O. Stelzer-Chilton,³⁴ D. Stentz,³⁹ J. Strogas,³⁸ G.L. Strycker,³⁵ J.S. Suh,²⁸ A. Sukhanov,¹⁹ I. Suslov,¹⁶ A. Taffard^{f,25} R. Takashima,⁴¹ Y. Takeuchi,⁵⁶ R. Tanaka,⁴¹ J. Tang,¹⁴ M. Tecchio,³⁵ P.K. Teng,¹ J. Thom^{h,18} J. Thome,¹³ G.A. Thompson,²⁵ E. Thomson,⁴⁶ P. Tipton,⁶¹ P. Ttito-Guzmán,³² S. Tkaczyk,¹⁸ D. Toback,⁵⁴ S. Tokar,¹⁵ K. Tollefson,³⁶ T. Tomura,⁵⁶ D. Tonelli,¹⁸ S. Torre,²⁰ D. Torretta,¹⁸ P. Totaro^{ii,55} S. Tourneur,⁴⁵ M. Trovato^{gg,47} S.-Y. Tsai,¹ Y. Tu,⁴⁶ N. Turini^{ff,47} F. Ukegawa,⁵⁶ S. Uozumi,²⁸ N. van Remortel^{b,24} A. Varganov,³⁵ E. Vataga^{gg,47} F. Vázquez^{n,19} G. Velez,¹⁸ C. Vellidis,³ M. Vidal,³² I. Vila,¹² R. Vilar,¹² M. Vogel,³⁸ I. Volobouev^{w,29} G. Volpi^{ee,47} P. Wagner,⁴⁶ R.G. Wagner,² R.L. Wagner,¹⁸ W. Wagner^{aa,27} J. Wagner-Kuhr,²⁷ T. Wakisaka,⁴² R. Wallny,⁹ S.M. Wang,¹ A. Warburton,³⁴ D. Waters,³¹ M. Weinberger,⁵⁴ J. Weinelt,²⁷ W.C. Wester III,¹⁸ B. Whitehouse,⁵⁷ D. Whiteson^{f,46} A.B. Wicklund,² E. Wicklund,¹⁸ S. Wilbur,¹⁴ G. Williams,³⁴ H.H. Williams,⁴⁶ P. Wilson,¹⁸ B.L. Winer,⁴⁰ P. Wittich^{h,18} S. Wolbers,¹⁸ C. Wolfe,¹⁴ H. Wolfe,⁴⁰ T. Wright,³⁵ X. Wu,²¹ F. Würthwein,¹⁰ A. Yagil,¹⁰ K. Yamamoto,⁴² J. Yamaoka,¹⁷ U.K. Yang^{r,14} Y.C. Yang,²⁸ W.M. Yao,²⁹ G.P. Yeh,¹⁸ K. Yi^{o,18} J. Yoh,¹⁸ K. Yorita,⁵⁸ T. Yoshida^{l,42} G.B. Yu,¹⁷ I. Yu,²⁸ S.S. Yu,¹⁸ J.C. Yun,¹⁸ A. Zanetti,⁵⁵ Y. Zeng,¹⁷ X. Zhang,²⁵ Y. Zheng^{d,9} and S. Zucchelli^{cc6}

(CDF Collaboration[†])

¹*Institute of Physics, Academia Sinica, Taipei, Taiwan 11529, Republic of China*

²*Argonne National Laboratory, Argonne, Illinois 60439*

³*University of Athens, 157 71 Athens, Greece*

⁴*Institut de Fisica d'Altes Energies, Universitat Autònoma de Barcelona, E-08193, Bellaterra (Barcelona), Spain*

⁵*Baylor University, Waco, Texas 76798*

⁶*Istituto Nazionale di Fisica Nucleare Bologna, cc University of Bologna, I-40127 Bologna, Italy*

⁷*Brandeis University, Waltham, Massachusetts 02254*

⁸*University of California, Davis, Davis, California 95616*

⁹*University of California, Los Angeles, Los Angeles, California 90024*

¹⁰*University of California, San Diego, La Jolla, California 92093*

¹¹*University of California, Santa Barbara, Santa Barbara, California 93106*

¹²*Instituto de Fisica de Cantabria, CSIC-University of Cantabria, 39005 Santander, Spain*

¹³*Carnegie Mellon University, Pittsburgh, PA 15213*

¹⁴*Enrico Fermi Institute, University of Chicago, Chicago, Illinois 60637*

¹⁵*Comenius University, 842 48 Bratislava, Slovakia; Institute of Experimental Physics, 040 01 Kosice, Slovakia*

¹⁶*Joint Institute for Nuclear Research, RU-141980 Dubna, Russia*

¹⁷*Duke University, Durham, North Carolina 27708*

¹⁸*Fermi National Accelerator Laboratory, Batavia, Illinois 60510*

¹⁹*University of Florida, Gainesville, Florida 32611*

²⁰*Laboratori Nazionali di Frascati, Istituto Nazionale di Fisica Nucleare, I-00044 Frascati, Italy*

²¹*University of Geneva, CH-1211 Geneva 4, Switzerland*

²²*Glasgow University, Glasgow G12 8QQ, United Kingdom*

²³*Harvard University, Cambridge, Massachusetts 02138*

²⁴*Division of High Energy Physics, Department of Physics,*

University of Helsinki and Helsinki Institute of Physics, FIN-00014, Helsinki, Finland

²⁵*University of Illinois, Urbana, Illinois 61801*

²⁶*The Johns Hopkins University, Baltimore, Maryland 21218*

²⁷*Institut für Experimentelle Kernphysik, Karlsruhe Institute of Technology, D-76131 Karlsruhe, Germany*

- ²⁸Center for High Energy Physics: Kyungpook National University, Daegu 702-701, Korea; Seoul National University, Seoul 151-742, Korea; Sungkyunkwan University, Suwon 440-746, Korea; Korea Institute of Science and Technology Information, Daejeon 305-806, Korea; Chonnam National University, Gwangju 500-757, Korea; Chonbuk National University, Jeonju 561-756, Korea
- ²⁹Ernest Orlando Lawrence Berkeley National Laboratory, Berkeley, California 94720
- ³⁰University of Liverpool, Liverpool L69 7ZE, United Kingdom
- ³¹University College London, London WC1E 6BT, United Kingdom
- ³²Centro de Investigaciones Energeticas Medioambientales y Tecnologicas, E-28040 Madrid, Spain
- ³³Massachusetts Institute of Technology, Cambridge, Massachusetts 02139
- ³⁴Institute of Particle Physics: McGill University, Montréal, Québec, Canada H3A 2T8; Simon Fraser University, Burnaby, British Columbia, Canada V5A 1S6; University of Toronto, Toronto, Ontario, Canada M5S 1A7; and TRIUMF, Vancouver, British Columbia, Canada V6T 2A3
- ³⁵University of Michigan, Ann Arbor, Michigan 48109
- ³⁶Michigan State University, East Lansing, Michigan 48824
- ³⁷Institution for Theoretical and Experimental Physics, ITEP, Moscow 117259, Russia
- ³⁸University of New Mexico, Albuquerque, New Mexico 87131
- ³⁹Northwestern University, Evanston, Illinois 60208
- ⁴⁰The Ohio State University, Columbus, Ohio 43210
- ⁴¹Okayama University, Okayama 700-8530, Japan
- ⁴²Osaka City University, Osaka 588, Japan
- ⁴³University of Oxford, Oxford OX1 3RH, United Kingdom
- ⁴⁴Istituto Nazionale di Fisica Nucleare, Sezione di Padova-Trento, ^{dd}University of Padova, I-35131 Padova, Italy
- ⁴⁵LPNHE, Universite Pierre et Marie Curie/IN2P3-CNRS, UMR7585, Paris, F-75252 France
- ⁴⁶University of Pennsylvania, Philadelphia, Pennsylvania 19104
- ⁴⁷Istituto Nazionale di Fisica Nucleare Pisa, ^{ee}University of Pisa, ^{ff}University of Siena and ^{gg}Scuola Normale Superiore, I-56127 Pisa, Italy
- ⁴⁸University of Pittsburgh, Pittsburgh, Pennsylvania 15260
- ⁴⁹Purdue University, West Lafayette, Indiana 47907
- ⁵⁰University of Rochester, Rochester, New York 14627
- ⁵¹The Rockefeller University, New York, New York 10021
- ⁵²Istituto Nazionale di Fisica Nucleare, Sezione di Roma 1, ^{hh}Sapienza Università di Roma, I-00185 Roma, Italy
- ⁵³Rutgers University, Piscataway, New Jersey 08855
- ⁵⁴Texas A&M University, College Station, Texas 77843
- ⁵⁵Istituto Nazionale di Fisica Nucleare Trieste/Udine, I-34100 Trieste, ⁱⁱUniversity of Trieste/Udine, I-33100 Udine, Italy
- ⁵⁶University of Tsukuba, Tsukuba, Ibaraki 305, Japan
- ⁵⁷Tufts University, Medford, Massachusetts 02155
- ⁵⁸Waseda University, Tokyo 169, Japan
- ⁵⁹Wayne State University, Detroit, Michigan 48201
- ⁶⁰University of Wisconsin, Madison, Wisconsin 53706
- ⁶¹Yale University, New Haven, Connecticut 06520

We report a measurement of the lifetime of the Λ_b^0 baryon in decays to the $\Lambda_c^+ \pi^-$ final state in a sample corresponding to 1.1 fb^{-1} collected in $p\bar{p}$ collisions at $\sqrt{s} = 1.96 \text{ TeV}$ by the CDF II detector at the Tevatron collider. Using a sample of about 3000 fully reconstructed Λ_b^0 events we measure $\tau(\Lambda_b^0) = 1.401 \pm 0.046 \text{ (stat)} \pm 0.035 \text{ (syst)} \text{ ps}$ (corresponding to $c\tau(\Lambda_b^0) = 420.1 \pm 13.7 \text{ (stat)} \pm 10.6 \text{ (syst)} \mu\text{m}$, where c is the speed of light). The ratio of this result and the world average B^0 lifetime yields $\tau(\Lambda_b^0)/\tau(B^0) = 0.918 \pm 0.038 \text{ (stat and syst)}$, in good agreement with recent theoretical predictions.

PACS numbers: 14.20.Mr, 13.30.-a, 12.39.Hg

*Deceased

†With visitors from ^aUniversity of Massachusetts Amherst, Amherst, Massachusetts 01003, ^bUniversiteit Antwerpen, B-2610 Antwerp, Belgium, ^cUniversity of Bristol, Bristol BS8 1TL,

United Kingdom, ^dChinese Academy of Sciences, Beijing 100864, China, ^eIstituto Nazionale di Fisica Nucleare, Sezione di Cagliari, 09042 Monserrato (Cagliari), Italy, ^fUniversity of California Irvine, Irvine, CA 92697, ^gUniversity of California Santa Cruz,

In the decays of beauty to charm hadrons the fundamental force underlying the decay of a b quark to a c quark is the weak interaction. However, the heavy b quark is surrounded by a cloud of light quarks and gluons so the strong interaction must be taken into account. In the limit of an infinite mass of the b quark, the heavy quark decouples from the light degrees of freedom. For a finite m_b the decay rates can be computed as a series expanded in the small parameter Λ_{QCD}/m_b , where m_b is the mass of the b quark and Λ_{QCD} is the energy scale of the QCD interactions within the hadron. This is known as the heavy-quark expansion (HQE) [1]. The application of HQE to the decays of the Λ_b^0 baryon (udb) and the beauty mesons ($B^0, \bar{b}d; B^+, \bar{b}u$) does not result in an identical series. For example, in the $(\Lambda_{QCD}/m_b)^3$ term W -boson exchange contributions are quite different [2], leading to a prediction of $\tau(\Lambda_b^0)/\tau(B^0) \neq 1$. Experimental studies of beauty hadron lifetimes therefore help us to test the theoretical understanding of the HQE series, and consequently the underlying QCD physics.

Over the past five years theoretical predictions of the lifetime ratio $\tau(\Lambda_b^0)/\tau(B^0)$ have not agreed with experimental values. In 2004 an HQE calculation including $\mathcal{O}(1/m_b^4)$ effects resulted in $\tau(\Lambda_b^0)/\tau(B^0) = 0.86 \pm 0.05$ [3]. This was in good agreement with the 2006 experimental world average of 0.804 ± 0.049 [4]. In 2006 the CDF collaboration reported a measurement [5] of the Λ_b^0 lifetime in the $\Lambda_b^0 \rightarrow J/\psi \Lambda^0$ channel such that $\tau(\Lambda_b^0)/\tau(B^0)$ differed by $+2\sigma$ from the 2006 world average [4], was significantly higher than the 2004 HQE calculation [3], but was compatible with earlier HQE predictions [6]. A more recent measurement by the $D\bar{O}$ collaboration [7] in the same channel leads to a value of $\tau(\Lambda_b^0)/\tau(B^0)$ which is compatible with both the 2006 world average [4] and the CDF value [5].

In this paper we present the first measurement of the Λ_b^0 lifetime in a fully hadronic final state. The data sam-

ple is produced in $p\bar{p}$ collisions at $\sqrt{s} = 1.96$ TeV at the Tevatron and corresponds to an integrated luminosity of 1.1 fb^{-1} . We reconstruct Λ_b^0 in the $\Lambda_b^0 \rightarrow \Lambda_c^+ \pi^-$ decay channel where Λ_c^+ subsequently decays as $\Lambda_c^+ \rightarrow pK^- \pi^+$. Throughout the paper, reference to a specific charge state also implies the charge conjugate state.

The components of the CDF II detector [8] most relevant for this analysis are the tracking system and the displaced vertex trigger system. The tracking system lies within a uniform axial magnetic field of 1.4 T. The inner tracking volume is instrumented with either 6 or 7 layers of double-sided silicon microstrip detectors up to a radius of 28 cm from the beamline [9]. These surround a layer of single-sided silicon mounted directly on the beam pipe at a radius of 1.5 cm [10]. This system provides an excellent resolution (about $40 \mu\text{m}$) on the impact parameter (d_0), which is defined as the distance of closest approach of the charged particle to the $p\bar{p}$ interaction point in the plane transverse to the beam direction. The d_0 resolution of $40 \mu\text{m}$ includes an approximate $30 \mu\text{m}$ contribution from the uncertainty of the interaction point in the transverse plane (added in quadrature). The outer tracking volume contains an open-cell drift chamber (COT) up to the radius of 137 cm [11].

CDF II employs a three-level trigger system. The extremely fast tracker (XFT) [12] at the first level groups COT hits into tracks in the transverse plane. At the second level, the silicon vertex trigger (SVT) [13] adds silicon hits to the tracks found by the XFT, improving the resolution of the track position and thus allowing selection based on the transverse displacement from the beam line that is measured in real time. The displaced vertex trigger [14] requires two charged particles with momentum transverse to the beam direction (p_T) greater than 2 GeV/ c , and with impact parameters in the range $0.12 < |d_0| < 1$ mm. The intersection point of the two particle trajectories must have a transverse displacement (L_{xy}) from the interaction point of at least $200 \mu\text{m}$. The pair must also have a scalar sum $p_T(1) + p_T(2) > 5.5$ GeV/ c . This trigger configuration based on a pair of tracks is called the two-track trigger (TTT) and is the basis for the collection of many fully hadronic bottom and charm decays at CDF.

We reconstruct a Λ_b^0 candidate via its decay to $\Lambda_c^+ \pi^-$, where the Λ_c^+ further decays to a $pK^- \pi^+$ final state. All four tracks are required to have a sufficient number of hits in the tracking detectors for high-quality position measurement. Several requirements are imposed to suppress background in the reconstructed sample which are optimized using simulated signal and data background samples [15]. Each particle must have $|d_0| < 1000 \mu\text{m}$. We construct Λ_c^+ candidates by combining three tracks assuming the $(pK^- \pi^+)$ hypothesis. The p candidate and the π^- are required to have $p_T > 2.0$ GeV/ c . The proton p_T must exceed the p_T of the π^+ from the Λ_c^+ , which has the same charge. This prevents the same pair of

Santa Cruz, CA 95064, ^hCornell University, Ithaca, NY 14853, ⁱUniversity of Cyprus, Nicosia CY-1678, Cyprus, ^jUniversity College Dublin, Dublin 4, Ireland, ^kUniversity of Edinburgh, Edinburgh EH9 3JZ, United Kingdom, ^lUniversity of Fukui, Fukui City, Fukui Prefecture, Japan 910-0017 ^mKinki University, Higashi-Osaka City, Japan 577-8502 ⁿUniversidad Iberoamericana, Mexico D.F., Mexico, ^oUniversity of Iowa, Iowa City, IA 52242, ^pKansas State University, Manhattan, KS 66506 ^qQueen Mary, University of London, London, E1 4NS, England, ^rUniversity of Manchester, Manchester M13 9PL, England, ^sMuons, Inc., Batavia, IL 60510, ^tNagasaki Institute of Applied Science, Nagasaki, Japan, ^uUniversity of Notre Dame, Notre Dame, IN 46556, ^vUniversity of Oviedo, E-33007 Oviedo, Spain, ^wTexas Tech University, Lubbock, TX 79609, ^xIFIC(CSIC-Universitat de Valencia), 56071 Valencia, Spain, ^yUniversidad Tecnica Federico Santa Maria, 110v Valparaiso, Chile, ^zUniversity of Virginia, Charlottesville, VA 22906 ^{aa}Bergische Universität Wuppertal, 42097 Wuppertal, Germany, ^{bb}Yarmouk University, Irbid 211-63, Jordan ^{jj}On leave from J. Stefan Institute, Ljubljana, Slovenia,

tracks being considered both as (p, π^+) and as (π^+, p) . The three tracks from the Λ_c^+ candidate are first constrained to a common vertex in a kinematic fit. Next we add a track and construct Λ_b^0 candidates through a further kinematic fit, which intersects the fourth track with the Λ_c^+ candidate trajectory. The mass of the Λ_c^+ candidate is constrained to the world average Λ_c^+ mass ($2.286 \text{ GeV}/c^2$) [16]. This second kinematic fit allows us to calculate $ct = L_{xy}cM/p_T$ and its uncertainty, σ_{ct} , where c is the speed of light, and t and M are the proper decay time and measured mass of the Λ_b^0 , respectively.

We apply additional selection requirements in order to suppress background. The requirements on $ct(\Lambda_b^0) > 250 \mu\text{m}$, its significance $ct(\Lambda_b^0)/\sigma_{ct} > 10$, and $|d_0(\Lambda_b^0)| < 80 \mu\text{m}$ primarily suppress the background arising from random combinations of tracks, many of which originate from the primary interaction point (combinatorial background). Another important source of background is the decay of B mesons with misidentified decay products. Decays like $\bar{B}^0 \rightarrow D^+\pi^-$ are especially insidious since they are abundant (compared to $\Lambda_b^0 \rightarrow \Lambda_c^+\pi^-$ decays) and $D^+ \rightarrow K^-\pi^+\pi^+$ decays can easily mimic the $\Lambda_c^+ \rightarrow K^-\pi^+\pi^+$ signature. These backgrounds are suppressed by selecting a narrow region of the invariant mass spectrum of the $\Lambda_c^+ \rightarrow pK^-\pi^+$ candidate: $|m(pK^-\pi^+) - m(\Lambda_c^+)_{PDG}| < 16 \text{ MeV}/c^2$. Further D^+ candidates are removed by a requirement on the ct of Λ_c^+ candidates with respect to the Λ_b^0 vertex, since the Λ_c^+ candidates are usually much shorter lived than the D^+ candidates. We require $-70 < ct(\Lambda_c^+ \text{ w.r.t. } \Lambda_b^0) < 200 \mu\text{m}$. Lastly, the TTT criteria are confirmed using the reconstructed candidate tracks.

The lifetime of the Λ_b^0 baryon is determined from two sequential maximum likelihood fits. The first is a fit to the invariant mass of $\Lambda_c^+\pi^-$ candidates and is used to establish the composition of the sample. This gives the normalization of each of the fit components for both the whole domain of $4.82 < m(\Lambda_b^0) < 7.0 \text{ GeV}/c^2$, as well as the signal region ($5.565 < m(\Lambda_b^0) < 5.670 \text{ GeV}/c^2$). The second fit is an unbinned maximum likelihood fit of ct and σ_{ct} in the signal region to extract the Λ_b^0 lifetime with the normalizations of each component fixed.

The invariant mass distribution of $\Lambda_c^+\pi^-$ candidates is shown in Fig. 1 with the fit projection overlaid. Small deviations of the model from data below the Λ_b^0 mass do not affect the lifetime as they occur outside the signal region. The $\Lambda_c^+\pi^-$ mass distribution is described by several components: the $\Lambda_b^0 \rightarrow \Lambda_c^+\pi^-$ signal, a combinatorial background, partially and fully reconstructed B mesons that pass the $\Lambda_c^+\pi^-$ selection criteria, partially reconstructed Λ_b^0 decays, and fully reconstructed Λ_b^0 decays other than $\Lambda_c^+\pi^-$ (e.g. $\Lambda_b^0 \rightarrow \Lambda_c^+K^-$). The combinatorial background is modeled with an exponentially decreasing function of $\Lambda_c^+\pi^-$ mass. All other components are represented in the fit by fixed shapes derived from Monte Carlo (MC) simulations [17] whose relative contributions

are constrained using data when possible. Significant differences between fit and data are only observed outside the signal region. The mass fit has $2905 \pm 58 \Lambda_b^0 \rightarrow \Lambda_c^+\pi^-$ signal events, 252 ± 46 other fully reconstructed Λ_b^0 candidates (which are also used to determine the Λ_b^0 lifetime), and 11% background in the signal region.

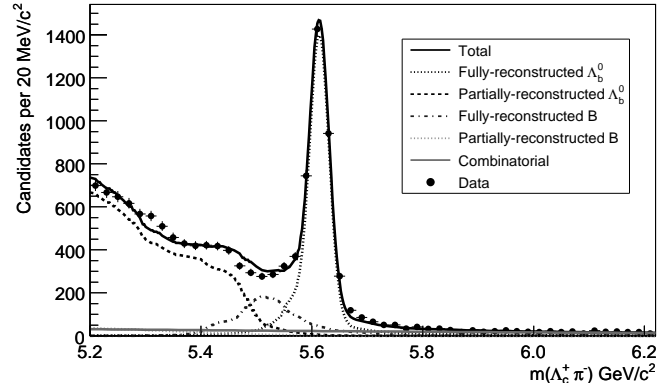


FIG. 1: The distribution of the invariant mass of $\Lambda_b^0 \rightarrow \Lambda_c^+\pi^-$ candidates (points) with the fit overlaid (solid black line).

Due to the trigger requirements on the track d_0 and track-pair L_{xy} , the observed Λ_b^0 ct distribution is not a simple exponential. Consequently, an efficiency ($\epsilon(ct)$) must be included to model the acceptance of the trigger and offline selection. The largest corrections are due to the d_0 requirements of the TTT. The two-dimensional $ct - \sigma_{ct}$ probability density function (pdf) for the signal and other fully reconstructed Λ_b^0 components is given by

$$P(ct, c\tau, \sigma_{ct}; S_{1,2}) = P(ct|c\tau, \sigma_{ct}, S_{1,2}) \cdot P(\sigma_{ct}) \cdot \epsilon(ct). \quad (1)$$

where $S_{1,2}$ are the two σ_{ct} scale factors obtained from a two-Gaussian modeling of the resolution function in MC (one for each Gaussian). The scale factor is necessary because the kinematic fitter underestimates the uncertainty on the ct (the same scale factor is used for signal and background). $P(ct|\sigma_{ct}, S_{1,2})$ is a one-dimensional conditional pdf for observing this value of ct given the true Λ_b^0 lifetime (τ), σ_{ct} , and $S_{1,2}$. For the fully reconstructed Λ_b^0 components this pdf is a decreasing exponential convoluted with the sum of the two resolution Gaussians. $P(\sigma_{ct})$ is the pdf for observing σ_{ct} and is obtained from the sideband subtracted data distribution, where the sideband is defined as $5.8 < m(\Lambda_b^0) < 7.0 \text{ GeV}/c^2$. For each background component Eq. 1 is modified in a suitable way, apart from the partially reconstructed B mesons, which do not populate the signal region and are therefore not included in the lifetime fit.

A sample of simulated signal events is used to extract $\epsilon(ct)$. This sample consists of single b hadrons generated with a p_T spectrum extracted from the data sample and decayed with EvtGen [18]. This MC sample is further reweighted in order to match the data in a number of relevant variables: the choice of ‘trigger tracks’

(the pair of final state particles which cause the TTT to fire), the proton production angle in Λ_c^+ rest frame which is sensitive to Λ_b^0 polarization, and the contributions of the Λ_c^+ Dalitz components [19]. The TTT efficiency function is represented by a histogram calculated as $\epsilon(ct) = h(ct) / \sum_i \exp(ct, c\tau^{MC}) \otimes R(S_{1,2}, \sigma_{ct}^i)$. The numerator is a smoothed histogram of the ct for all MC events that pass the trigger and analysis selection criteria. Each bin of the denominator is calculated by summing the analytical ct distribution at the ct bin center over all events (indexed by i) that pass the criteria required to fill the numerator. The analytical ct distribution is an exponential convoluted with the resolution function R . Fig. 2 shows the resulting finely binned TTT efficiency histogram used for the Λ_b^0 signal components. Exactly the same procedure was used to derive an efficiency histogram for the fully reconstructed B meson background.

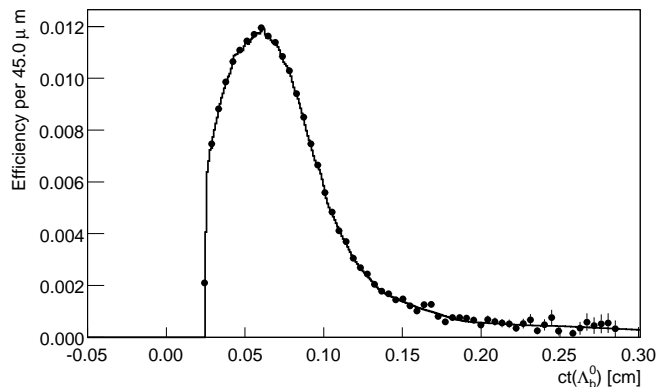


FIG. 2: The smoothed Λ_b^0 TTT efficiency histogram (line) superimposed on the unsmoothed histogram (points)

Our approach assumes that the simulation of trigger and detector can be used to derive $\epsilon(ct)$. This assumption can be validated in data using $J/\psi \rightarrow \mu^+\mu^-$ decays collected by the dimuon trigger which does not bias their lifetime. The observed four momenta of $J/\psi \rightarrow \mu^+\mu^-$ decays were also used as the input for a simulated sample of $J/\psi \rightarrow \mu^+\mu^-$ decays, subsequently fed to the TTT and detector simulation (data-seeded MC). Comparing the number of real $J/\psi \rightarrow \mu^+\mu^-$ decays that pass the TTT with the number of data-seeded simulation decays that pass the TTT simulation gives a direct check of the reliability of the simulation. For both real and simulated J/ψ decays we compute the TTT efficiency as a function of L_{xy} and form their ratio $R_\epsilon(L_{xy})$. The deviation of the slope of $R_\epsilon(L_{xy})$ from 0 is a measure of the quality of modeling of TTT in the simulation. Observed $R_\epsilon(L_{xy})$ is incompatible with a null slope at the $3-4\sigma$ level; we treat this discrepancy as a source of systematic uncertainty.

We perform an unbinned maximum likelihood fit for $c\tau(\Lambda_b^0)$ to the data that yields $c\tau(\Lambda_b^0) = 420.1 \pm 13.7 \mu\text{m}$ (stat). The total likelihood is: $\mathcal{L} = \prod_i \sum_j N_j^{\text{sig}} \cdot P_j(ct_i, \sigma_{ct i}; S_{1,2})$, where the subscript i runs over events,

and the subscript j runs over classes of event: the fully reconstructed signal and background fit components, the combinatorial background, and the partially reconstructed Λ_b^0 decays. $P_j(ct_i, \sigma_{ct i}; S_{1,2})$ is a two-dimensional pdf of the form given in Eq. 1, N_j^{sig} is the number of events of this class occurring in the signal region. The resulting likelihood projected onto the ct -axis is shown in Fig. 3. We fit the data for the Λ_b^0 lifetime after all procedures are established. The fit probability is estimated to be 37% using an unbinned Kolmogorov-Smirnov test.

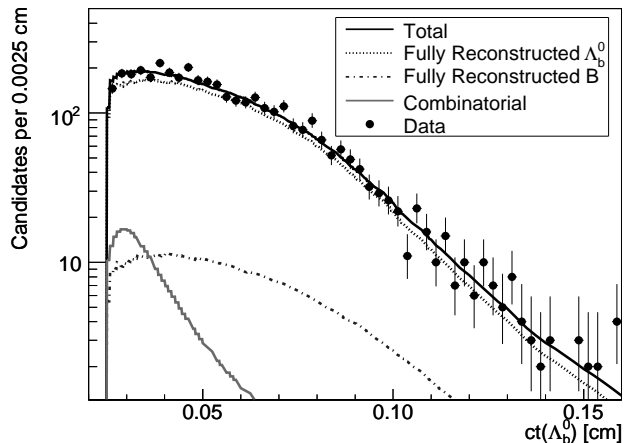


FIG. 3: The distribution of the ct of $\Lambda_b^0 \rightarrow \Lambda_c^+ \pi^-$ candidates (points) with the fit projection overlaid (solid black line). The partially reconstructed Λ_b^0 fit components only have a 1% contribution to the signal region and are not shown.

For each source of systematic uncertainty, we generate sets of events for about 500 pseudo experiments from a modified pdf and fit with both the standard and modified fits. The mean of the distribution of the difference between fit results obtained with the standard and modified pdf is used as the systematic uncertainty. We consider the systematic uncertainties in two groups based on whether they affect the TTT efficiency or not.

In the first group, the systematic uncertainty due to the alignment of the silicon detector is quoted from a previous study [5] ($2.0 \mu\text{m}$) where internal silicon sensor deformations and global misalignments of the silicon detector relative to the outer tracking volume are taken into account. The uncertainty due to the background component normalizations was taken into account by varying them according to their uncertainties derived from the mass fit ($1.0 \mu\text{m}$).

In the second group of uncertainties, where the TTT efficiency is directly affected, the leading source is due to the slope of $R_\epsilon(L_{xy})$ ($8.6 \mu\text{m}$). The uncertainty due to the Λ_c^+ Dalitz structure is evaluated by varying the relative contributions of each Dalitz component according to the world average uncertainty [16] ($3.7 \mu\text{m}$). The effect of an uncertainty in the combina-

torial background ct template is computed by modifying it to a smoothed version of the actual upper sideband ct distribution ($2.9 \mu\text{m}$). The uncertainty due to the particle identity of the tracks which fired the trigger is evaluated by varying the relative contributions of different trigger-track combinations in the MC ($2.0 \mu\text{m}$). The uncertainty due to the Λ_b^0 polarization is obtained by varying the slope of the MC reweighting factor by one-sigma from a straight line fit for the proton production angle in the Λ_c^+ rest frame ($1.4 \mu\text{m}$). The uncertainty due to the transverse position of the $p\bar{p}$ primary interaction point is computed by dividing the MC into independent subsamples representing the extreme variations of the primary interaction point ($1.2 \mu\text{m}$). The uncertainty due to the TTT efficiency used for the B^0 background is evaluated by tightening the mass cut on the $D^+\pi^-$ candidate in the underlying B^0 MC reconstruction ($1.0 \mu\text{m}$). The uncertainty due to the lifetime assumed for the B^0 background is obtained by varying this lifetime according to the world average uncertainty [16] ($1.0 \mu\text{m}$). The uncertainty due to a correlation between the d_0 requirements in the SVT and reconstruction levels is estimated by smearing the latter in the signal MC by an amount extracted by comparing their difference distributions between data and MC ($1.0 \mu\text{m}$). The total systematic uncertainty is computed by adding all the contributions in quadrature, which is $10.6 \mu\text{m}$.

Numerous cross-checks were performed. We used our procedure to measure the B^0 lifetime in the $B^0 \rightarrow D^{*-}\pi^+$ and $B^0 \rightarrow D^-\pi^+$ decay modes and the B^+ lifetime in the $B^+ \rightarrow \bar{D}^0\pi^+$ mode. These B^0 and B^+ lifetime measurements are statistically consistent with the world averages [16]. We checked the effect of uncertainties in the mass template shapes, the p_T spectrum of the Λ_b^0 , the effect of assuming different Λ_b^0 lifetimes in the MC, the scale factor applied to the σ_{ct} , the Λ_c^+ lifetime, and the model of the uncertainty of the transverse position of the $p\bar{p}$ primary interaction point. We also checked the effect of the uncertainty in the shape of σ_{ct} and used a large signal MC sample to verify that the fitter itself does not introduce a bias in the measured lifetime.

In summary, using a sample of 2905 ± 58 fully reconstructed $\Lambda_b^0 \rightarrow \Lambda_c^+\pi^-$ decays we measure the lifetime of the Λ_b^0 baryon to be $\tau(\Lambda_b^0) = 1.401 \pm 0.046$ (stat) ± 0.035 (syst) ps (corresponding to $c\tau(\Lambda_b^0) = 420.1 \pm 13.7$ (stat) ± 10.6 (syst) μm where c is the speed of light). This is the single most precise measurement of the Λ_b^0 lifetime.

Using the current world average for the B^0 lifetime [16], we obtain $\tau(\Lambda_b^0)/\tau(B^0) = 0.918 \pm 0.038$ (stat + syst). There is good agreement between our result and the current world average of $\tau(\Lambda_b^0)/\tau(B^0) = 0.99 \pm 0.10$ [16], and between our result and the previous CDF result [5]. This measurement is also compatible with the current HQE value [3] of $\tau(\Lambda_b^0)/\tau(B^0) = 0.86 \pm 0.05$, thus supporting the HQE picture of weak decays of heavy

baryons.

We thank the Fermilab staff and the technical staffs of the participating institutions for their vital contributions. This work was supported by the U.S. Department of Energy and National Science Foundation; the Italian Istituto Nazionale di Fisica Nucleare; the Ministry of Education, Culture, Sports, Science and Technology of Japan; the Natural Sciences and Engineering Research Council of Canada; the National Science Council of the Republic of China; the Swiss National Science Foundation; the A.P. Sloan Foundation; the Bundesministerium für Bildung und Forschung, Germany; the World Class University Program, the National Research Foundation of Korea; the Science and Technology Facilities Council and the Royal Society, UK; the Institut National de Physique Nucleaire et Physique des Particules/CNRS; the Russian Foundation for Basic Research; the Ministerio de Ciencia e Innovación, and Programa Consolider-Ingenio 2010, Spain; the Slovak R&D Agency; and the Academy of Finland.

-
- [1] G. Bellini, I. I. Y. Bigi, and P. J. Dornan, Phys. Rept. **289**, 1 (1997).
 - [2] I. I. Y. Bigi, in Proceedings of 3rd International Conference On B Physics And CP Violation, Taipei, 2000.
 - [3] F. Gabbiani, A. I. Onishchenko, and A. A. Petrov, Phys. Rev. D **70**, 094031 (2004).
 - [4] W. M. Yao *et al.*, J. Phys. G **33**, 1 (2006).
 - [5] A. Abulencia *et al.* (CDF Collaboration), Phys. Rev. Lett. **98**, 122001 (2007).
 - [6] N. Uraltsev, Phys. Lett. **B376**, 303 (1996).
D. Pirjol and N. Uraltsev, Phys. Rev. D **59**, 034012 (1999).
P. Colangelo and F. De Fazio, Phys. Lett. B **387**, 371 (1996).
M. Di Pierro, C. Sachrajda, and C. Michael, Phys. Lett. B **468**, 143 (1999).
 - [7] V. M. Abazov *et al.* (DØ Collaboration), Phys. Rev. Lett. **99**, 142001 (2007).
 - [8] A. Abulencia *et al.* (CDF Collaboration), J. Phys. G **34**, 2457 (2007).
 - [9] A. Sill *et al.*, Nucl. Instrum. Methods A **447**, 1 (2000).
 - [10] C. S. Hill (on behalf of the CDF Collaboration), Nucl. Instrum. Methods A **530**, 1 (2004).
 - [11] A. Affolder *et al.* (CDF Collaboration), Nucl. Instrum. Methods A **526**, 249 (2004).
 - [12] E. J. Thomson *et al.*, IEEE Trans. Nucl. Sci. **49**, 1063 (2002).
 - [13] J. A. Adelman *et al.* (CDF Collaboration), Nucl. Instrum. Methods A **572**, 361 (2007).
 - [14] A. Abulencia *et al.* (CDF Collaboration), Phys. Rev. Lett. **98**, 122002 (2007).
 - [15] T. Aaltonen *et al.* (CDF Collaboration), Phys. Rev. Lett. **99**, 202001 (2007).
 - [16] C. Amsler *et al.*, Phys Lett B **667**, 1 (2008) and 2009 partial update for 2010 edition.
 - [17] We use a variety of single b hadron simulations, all using $p_T(B)$ distributions obtained from B decays in data

- (D. Acosta *et al.* (CDF Collaboration), Phys. Rev. D **71**, 032001 (2005)).
- [18] D. J. Lange, Nucl. Instrum. Methods A **462**, 152 (2001).
- [19] R. H. Dalitz, Phil. Mag. **44**, 1068 (1953).